

Ab-initio study of high-order harmonics and isolated attosecond pulses from a solid target: two-color pulse impact

Zahra Nourbakhsh, N. Tancogne-Dejean, H. Merdji, O. D. Mücke, and A. Rubio

Max Planck Institute for the Structure and Dynamics of Matter, Hamburg



online Women Physicists' Conference 2020

Hamburg University
5-7 November 2020



(A) Linearly polarized pulse

I. One-color vs two-color: Asymmetric pulse and IAPs

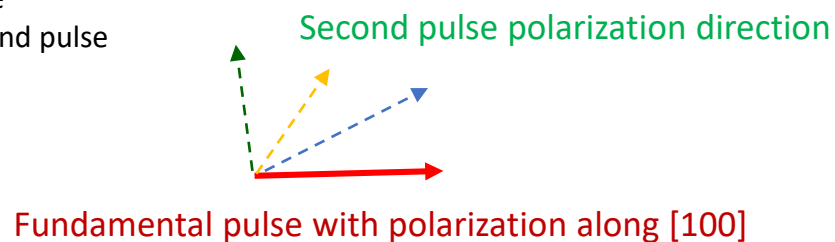
Localizing the pulse energy in a shorter area of pulse duration using asymmetric pulses, created by tuning the second pulse **frequency**, **intensity** and **phase difference**

II. Anisotropy impacts on HHG and IAPs

MgO crystal: combine advantages of both atomic and solid systems

(B) Non-linear polarized pulse: Ellipticity impacts on HHG and IAPs

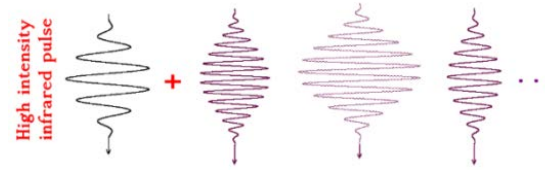
Generating customized elliptically polarized pulse by rotating the polarization direction of the second pulse



(A) Linearly polarized pulse

I. One-color vs two-color: Asymmetric pulse and IAPs

Localizing the pulse energy in a shorter area of pulse duration using asymmetric pulses, created by tuning the second pulse **frequency**, **intensity** and **phase difference**

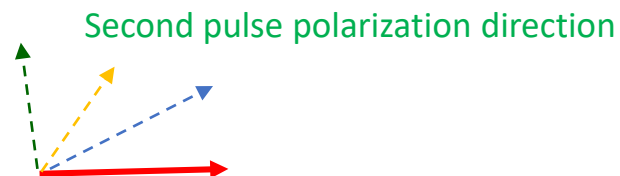


II. Anisotropy impacts on HHG and IAPs

MgO crystal: combine advantages of both atomic and solid systems

(B) Non-linear polarized pulse: Ellipticity impacts on HHG and IAPs

Generating customized elliptically polarized pulse
by rotating the polarization direction of the second pulse



Fundamental pulse with polarization along [100]

(A) Linearly polarized pulse

I. One-color vs two-color: Asymmetric pulse and IAPs

Localizing the pulse energy in a shorter area of pulse duration using asymmetric pulses, created by tuning the second pulse **frequency**, **intensity** and **phase difference**

II. Anisotropy impacts on HHG and IAPs

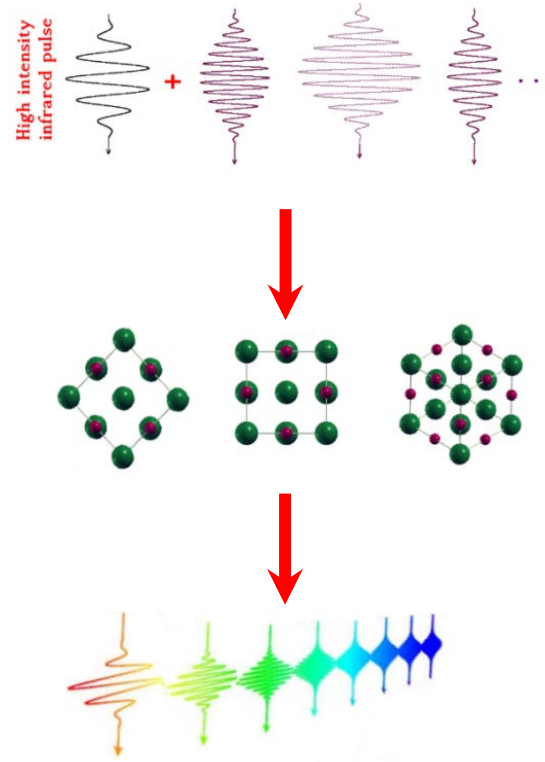
MgO crystal: combine advantages of both atomic and solid systems

Light-Matter interactions are simulated using **ab-initio TDDFT** framework with **Octopus** code on the basis of Kohn-Sham equation

$$i \frac{\partial}{\partial t} \phi_i(\vec{r}, t) = \left(-\frac{\nabla^2}{2} + \hat{v}_{ext}(\vec{r}, t) + \hat{v}_H[n(\vec{r}, t)] + \hat{v}_{xc}[n(\vec{r}, t)] \right) \phi_i(\vec{r}, t)$$

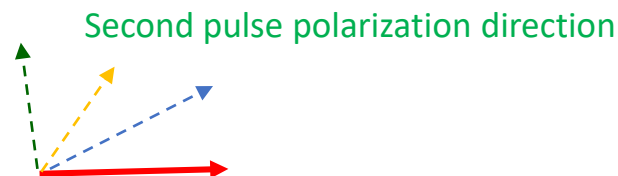
Self-consistent calculations

$$n(\vec{r}, t) = \sum_i |\phi_i(\vec{r}, t)|^2 \rightarrow i(t) \propto \int dr \frac{\partial n(r, t)}{\partial t}$$



(B) Non-linear polarized pulse: Ellipticity impacts on HHG and IAPs

Generating customized elliptically polarized pulse by rotating the polarization direction of the second pulse



Fundamental pulse with polarization along [100]

(A) Linearly polarized pulse

I. One-color vs two-color: Asymmetric pulse and IAPs

Localizing the pulse energy in a shorter area of pulse duration using asymmetric pulses, created by tuning the second pulse **frequency**, **intensity** and **phase difference**

II. Anisotropy impacts on HHG and IAPs

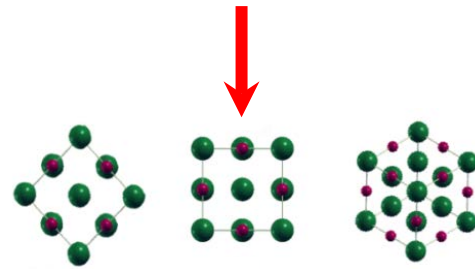
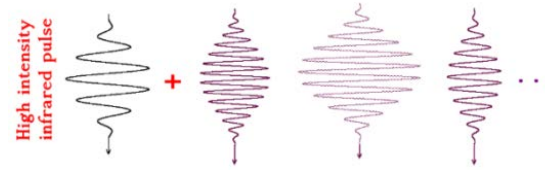
MgO crystal: combine advantages of both atomic and solid systems

Light-Matter interactions are simulated using **ab-initio TDDFT** framework with **Octopus** code on the basis of Kohn-Sham equation

$$i \frac{\partial}{\partial t} \phi_i(\vec{r}, t) = \left(-\frac{\nabla^2}{2} + \hat{v}_{ext}(\vec{r}, t) + \hat{v}_H[n(\vec{r}, t)] + \hat{v}_{xc}[n(\vec{r}, t)] \right) \phi_i(\vec{r}, t)$$

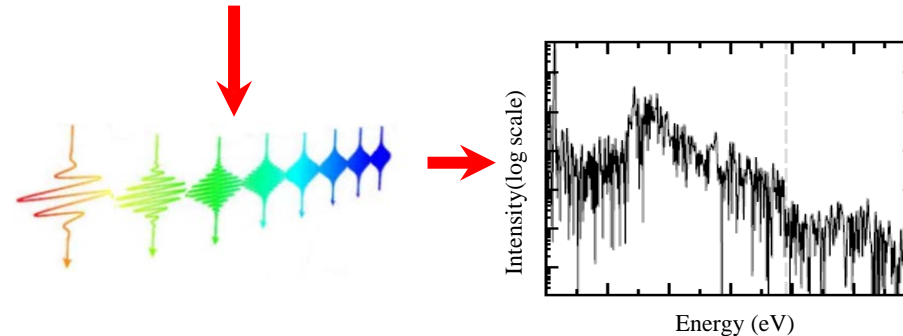
Self-consistent calculations

$$n(\vec{r}, t) = \sum_i |\phi_i(\vec{r}, t)|^2 \rightarrow i(t) \propto \int dr \frac{\partial n(r, t)}{\partial t}$$



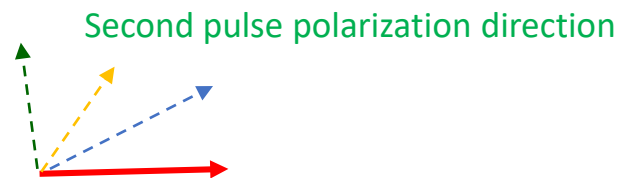
The first physical result:

$$HHG(\omega) = \left| FT \left(\frac{\partial i(t)}{\partial t} \right) \right|^2$$



(B) Non-linear polarized pulse: Ellipticity impacts on HHG and IAPs

Generating customized elliptically polarized pulse by rotating the polarization direction of the second pulse



Fundamental pulse with polarization along [100]

(A) Linearly polarized pulse

I. One-color vs two-color: Asymmetric pulse and IAPs

Localizing the pulse energy in a shorter area of pulse duration using asymmetric pulses, created by tuning the second pulse frequency, intensity and phase difference

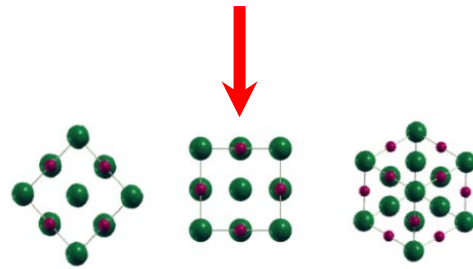
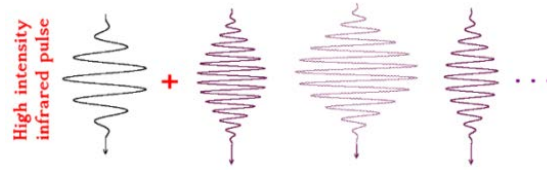
II. Anisotropy impacts on HHG and IAPs

MgO crystal: combine advantages of both atomic and solid systems

Light-Matter interactions are simulated using *ab-initio* TDDFT framework with Octopus code on the basis of Kohn-Sham equation

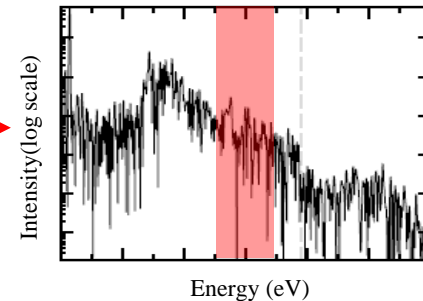
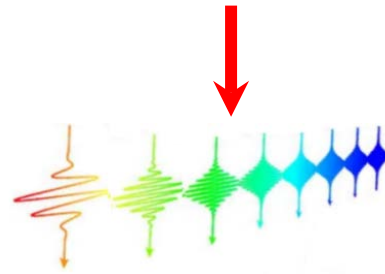
$$i \frac{\partial}{\partial t} \phi_i(\vec{r}, t) = \left(-\frac{\nabla^2}{2} + \hat{v}_{ext}(\vec{r}, t) + \hat{v}_H[n(\vec{r}, t)] + \hat{v}_{xc}[n(\vec{r}, t)] \right) \phi_i(\vec{r}, t)$$

Self-consistent calculations

$$n(\vec{r}, t) = \sum_i |\phi_i(\vec{r}, t)|^2 \rightarrow i(t) \propto \int dr \frac{\partial n(r, t)}{\partial t}$$


The first physical result:

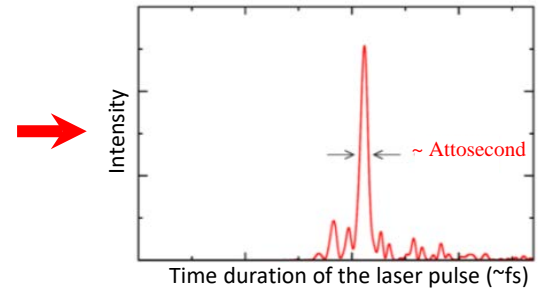
$$HHG(\omega) = \left| FT \left(\frac{\partial i(t)}{\partial t} \right) \right|^2$$



IAP Generation

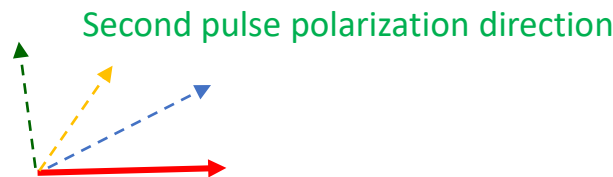
$$I(t) = \left| \sum_{\omega_i}^{\omega_f} FT \left(\frac{\partial i(t)}{\partial t} \right) \right|^2$$

IAPs can reveal microscopic details of the physical processes such as electron motion in materials, bond creation or bond breaking, and ultrafast, sub-optical-cycle, quantum mechanical phenomena



(B) Non-linear polarized pulse: Ellipticity impacts on HHG and IAPs

Generating customized elliptically polarized pulse by rotating the polarization direction of the second pulse



Fundamental pulse with polarization along [100]

(A) Linearly polarized pulse

I. One-color vs two-color: Asymmetric pulse and IAPs

Localizing the pulse energy in a shorter area of pulse duration using asymmetric pulses, created by tuning the second pulse frequency, intensity and phase difference

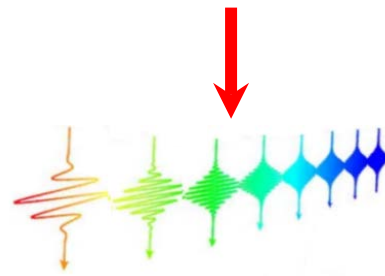
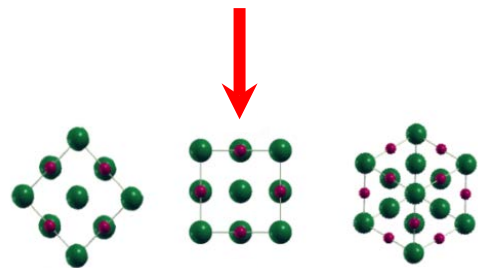
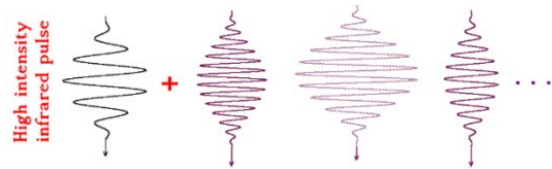
II. Anisotropy impacts on HHG and IAPs

MgO crystal: combine advantages of both atomic and solid systems

Light-Matter interactions are simulated using *ab-initio* TDDFT framework with Octopus code on the basis of Kohn-Sham equation

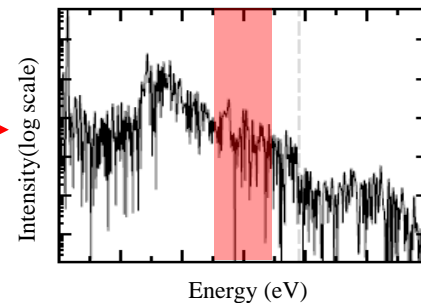
$$i \frac{\partial}{\partial t} \phi_i(\vec{r}, t) = \left(-\frac{\nabla^2}{2} + \hat{v}_{ext}(\vec{r}, t) + \hat{v}_H[n(\vec{r}, t)] + \hat{v}_{xc}[n(\vec{r}, t)] \right) \phi_i(\vec{r}, t)$$

Self-consistent calculations

$$n(\vec{r}, t) = \sum_i |\phi_i(\vec{r}, t)|^2 \rightarrow i(t) \propto \int dr \frac{\partial n(r, t)}{\partial t}$$


The first physical result:

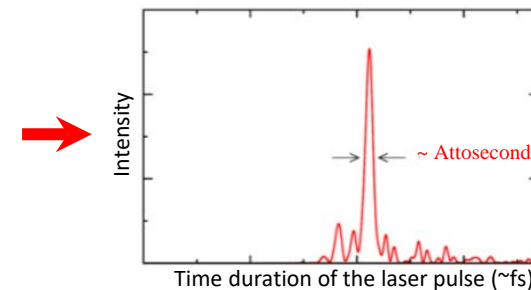
$$HHG(\omega) = \left| FT \left(\frac{\partial i(t)}{\partial t} \right) \right|^2$$



IAP Generation

$$I(t) = \left| \sum_{\omega_i}^{\omega_f} FT \left(\frac{\partial i(t)}{\partial t} \right) \right|^2$$

IAPs can reveal microscopic details of the physical processes such as electron motion in materials, bond creation or bond breaking, and ultrafast, sub-optical-cycle, quantum mechanical phenomena



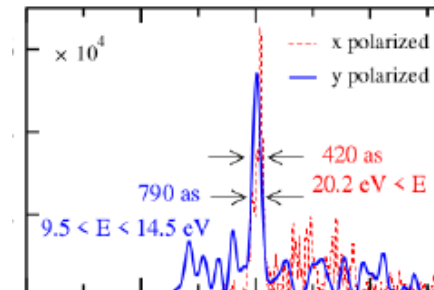
(B) Non-linear polarized pulse: Ellipticity impacts on HHG and IAPs

Generating customized elliptically polarized pulse by rotating the polarization direction of the second pulse

Second pulse polarization direction



Fundamental pulse with polarization along [100]



Generation of elliptical IAPs important for studying spin polarized electronic motion

Fundamental pulse properties

Applied pulse parameters:

$\lambda = 1800$ nm

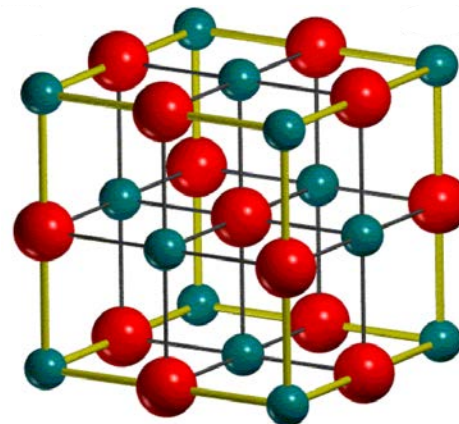
Vacuum intensity: 10^{13} W/cm² $\rightarrow E \approx 0.6$ V/Å

Pulse duration, full width at half maximum (FWHM): 18 fs

Laser electric field direction: [100]

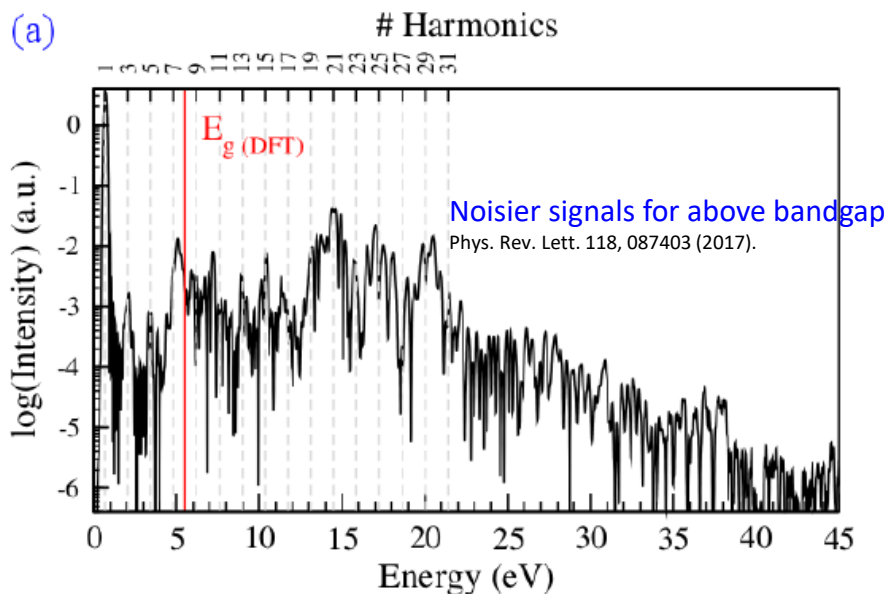
The pulse envelope shape: $\sin^2(t/\delta)$

MgO crystal (RS structure)

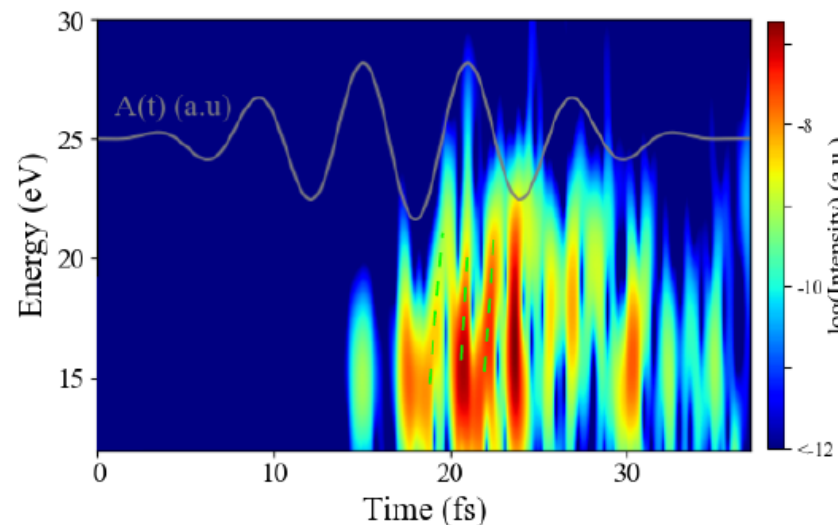


Electric field: Vector potential time derivative

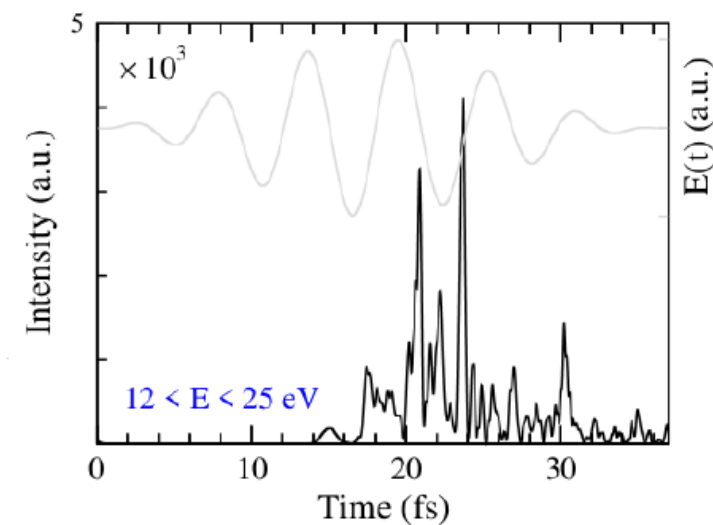
$$\vec{E}(t) = \frac{\partial}{\partial t} \vec{A}(t)$$



(b) The time-frequency analysis



(c) a train of attosecond pulses



Fundamental pulse properties

Applied pulse parameters:

$\lambda = 1800$ nm

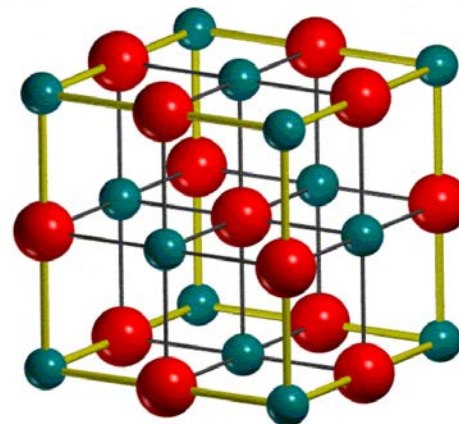
Vacuum intensity: 10^{13} W/cm² $\rightarrow E \approx 0.6$ V/Å

Pulse duration, full width at half maximum (FWHM): 18 fs

Laser electric field direction: [100]

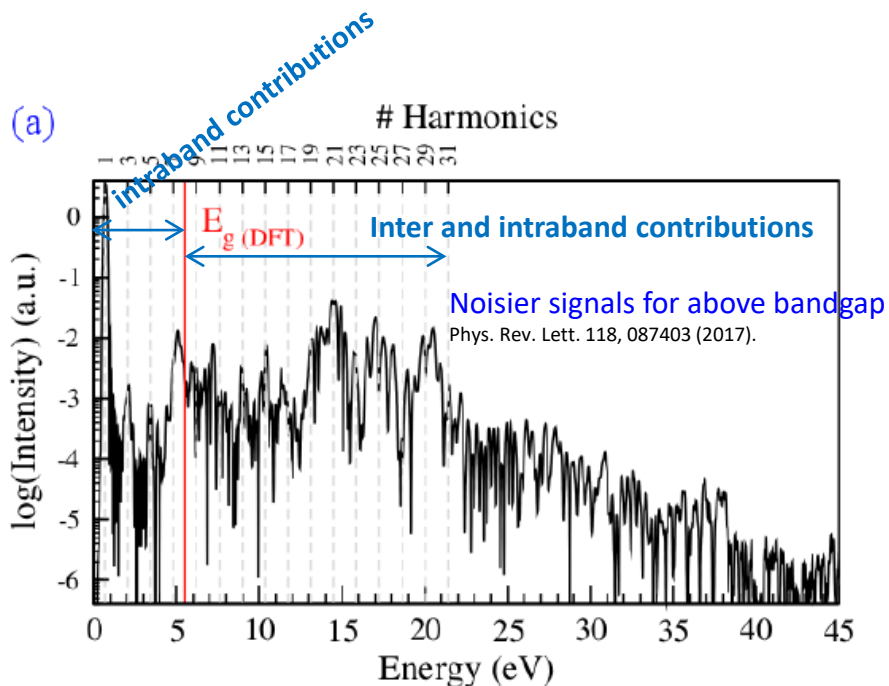
The pulse envelope shape: $\sin^2(t/\delta)$

MgO crystal (RS structure)

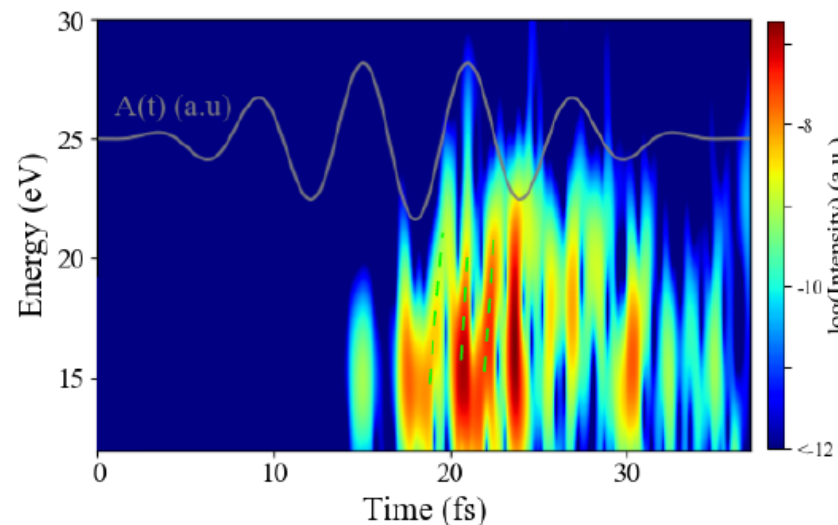


Electric field: Vector potential time derivative

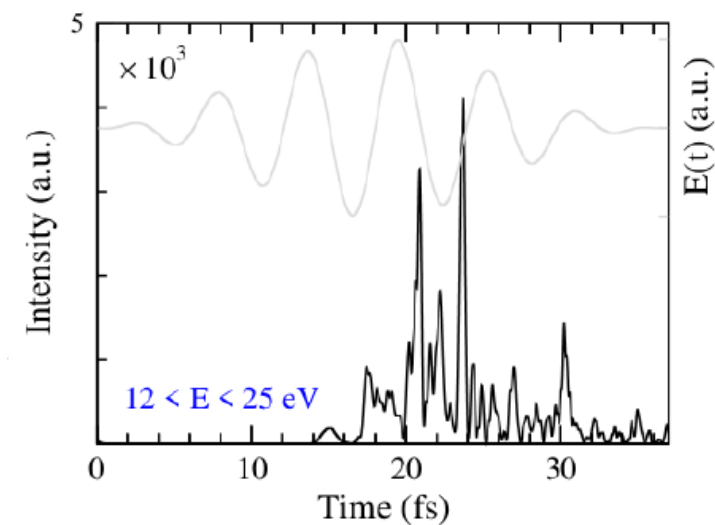
$$\vec{E}(t) = \frac{\partial}{\partial t} \vec{A}(t)$$



(b) The time-frequency analysis



(c) a train of attosecond pulses



Fundamental pulse properties

Applied pulse parameters:

$\lambda = 1800$ nm

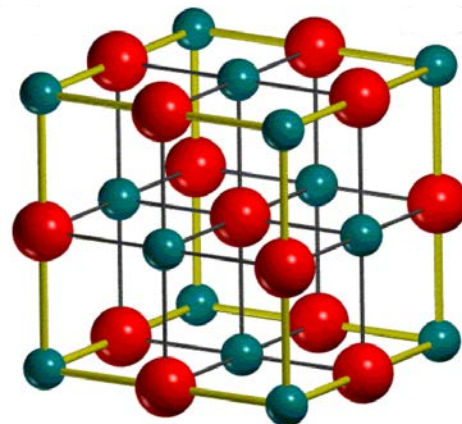
Vacuum intensity: 10^{13} W/cm² $\rightarrow E \approx 0.6$ V/Å

Pulse duration, full width at half maximum (FWHM): 18 fs

Laser electric field direction: [100]

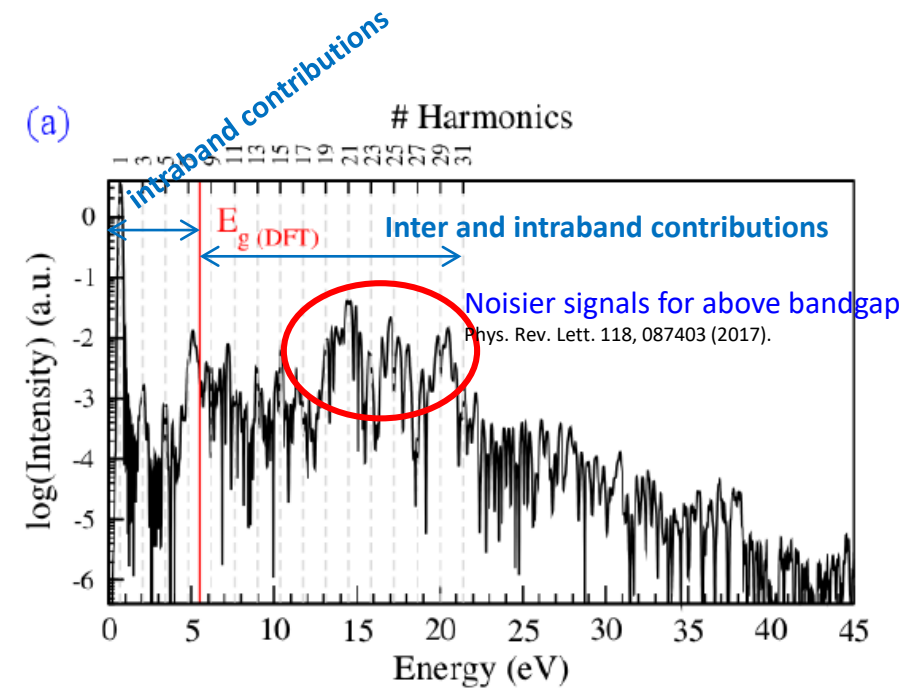
The pulse envelope shape: $\sin^2(t/\delta)$

MgO crystal (RS structure)

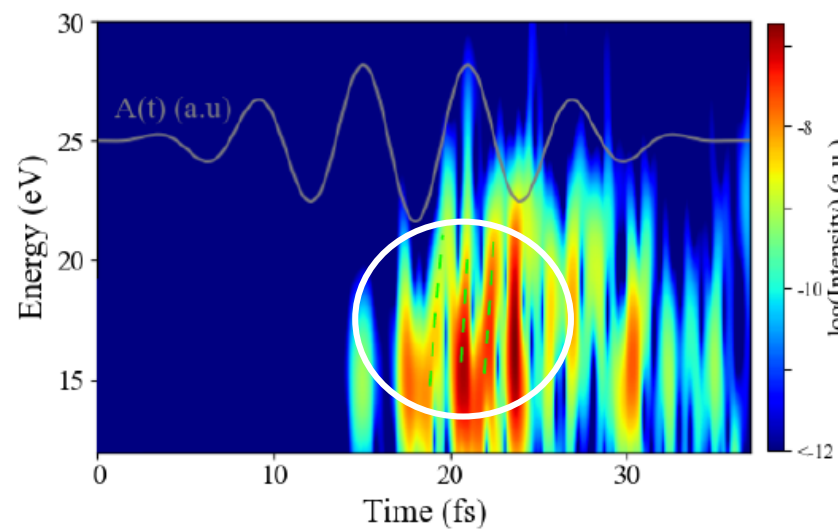


Electric field: Vector potential time derivative

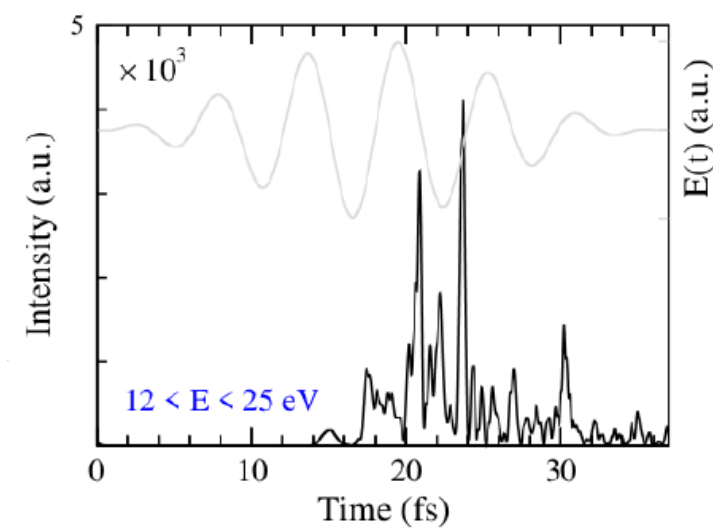
$$\vec{E}(t) = \frac{\partial}{\partial t} \vec{A}(t)$$



(b) The time-frequency analysis

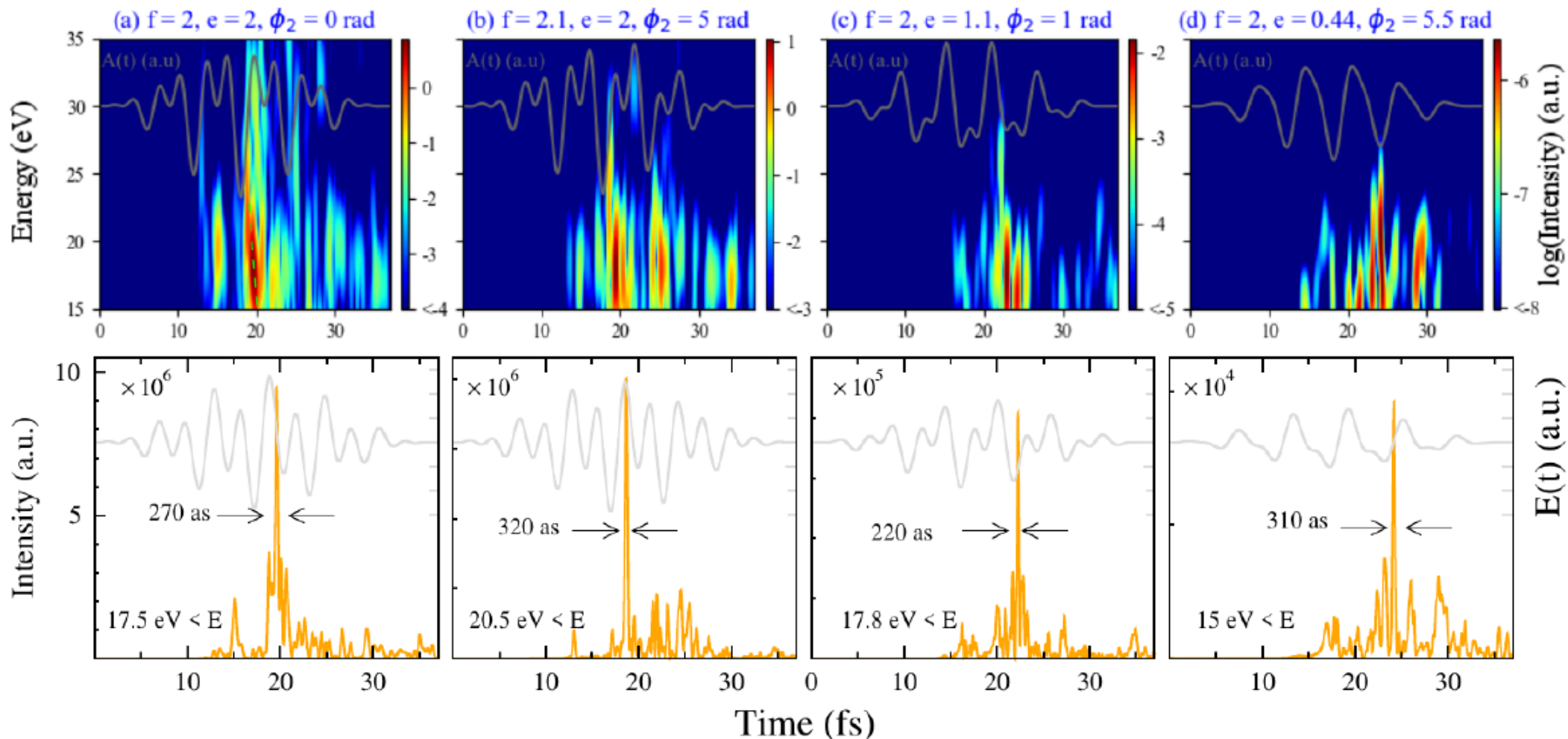


(c) a train of attosecond pulses



$$\vec{A}(t) = \vec{A}_0 \sin^2(t\pi/\delta) [\sin(\omega_0 t) + e/f \sin(f\omega_0 t + \phi_2)]$$

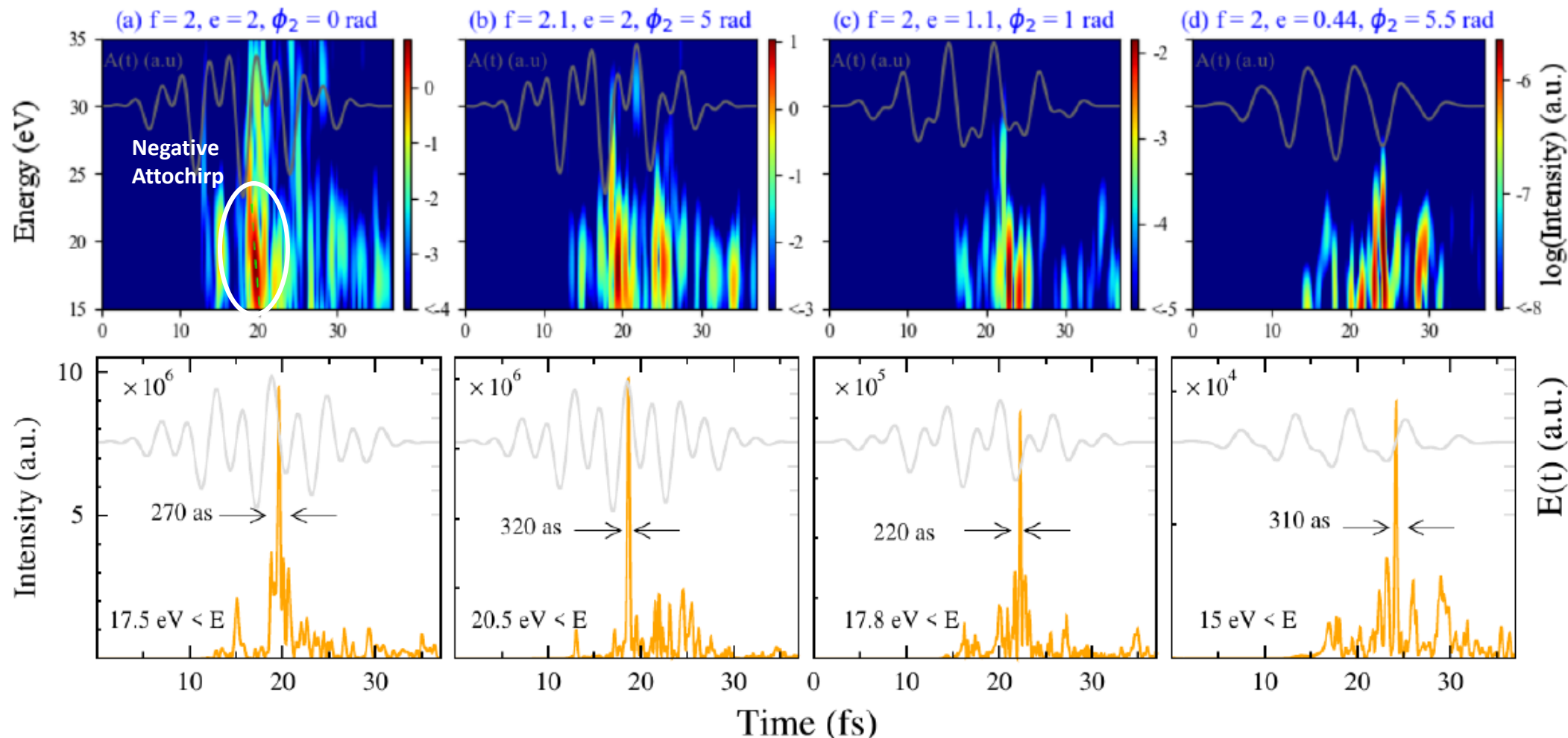
pulse shape and HHG spectra ← Second pulse strength, frequency and phase difference



- Using two-color intense pulses, IAPs of duration as short as \sim **200-300 as** are extracted from the harmonic emission in EUV range.
- Much shorter than what measured experimentally in SiO₂ nanofilm (**470 as**) [Nat. 538, 359] or the *ab initio* prediction of IAP duration in MoS₂ monolayer (**2280 as**) [APL 116, 043101].
- The energy windows to extract the IAPs are much wider than the calculated bandwidth in MoS₂ (**16-20 eV**) and that measured in SiO₂ (**18-28 eV**). For example, the filtering area in (a) starts from **17.5 eV** and cover the EUV energy range up to **43 eV**.

$$\vec{A}(t) = \vec{A}_0 \sin^2(t\pi/\delta) [\sin(\omega_0 t) + e/f \sin(f\omega_0 t + \phi_2)]$$

pulse shape and HHG spectra ← Second pulse strength, frequency and phase difference

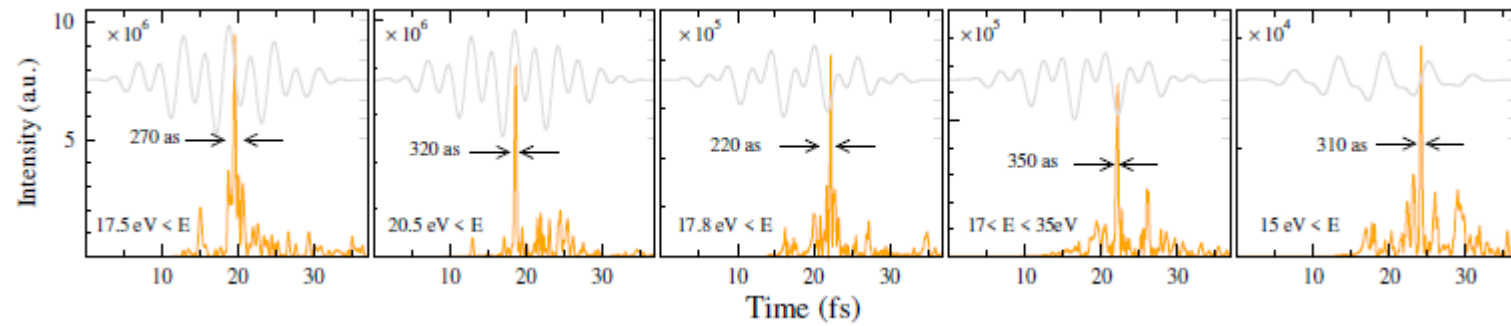
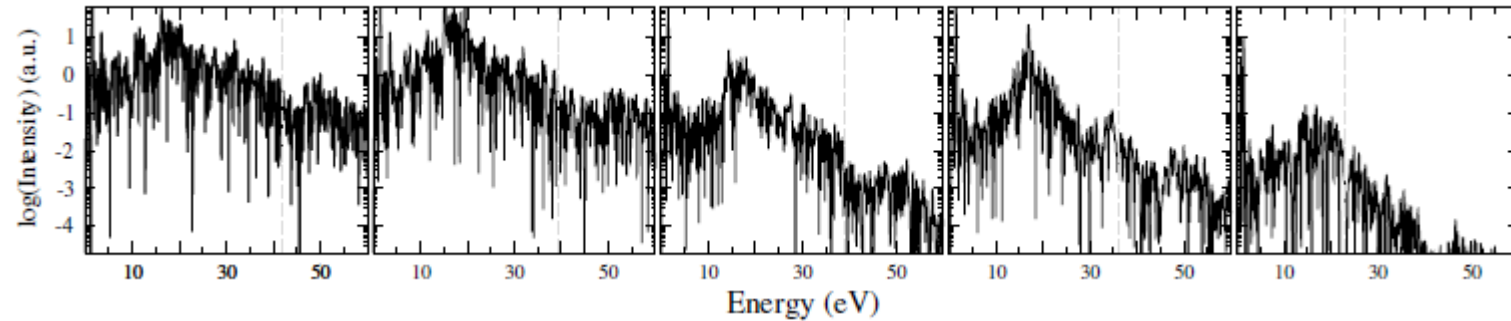


- Using two-color intense pulses, IAPs of duration as short as \sim **200-300 as** are extracted from the harmonic emission in EUV range.
- Much shorter than what measured experimentally in SiO₂ nanofilm (**470 as**) [Nat. 538, 359] or the *ab initio* prediction of IAP duration in MoS₂ monolayer (**2280 as**) [APL 116, 043101].
- The energy windows to extract the IAPs are much wider than the calculated bandwidth in MoS₂ (**16-20 eV**) and that measured in SiO₂ (**18-28 eV**). For example, the filtering area in (a) starts from **17.5 eV** and cover the EUV energy range up to **43 eV**.

two-color pulses

$E_{peak} = 1.7 \text{ V/\AA}$ ← increasing → 0.8 V/\AA

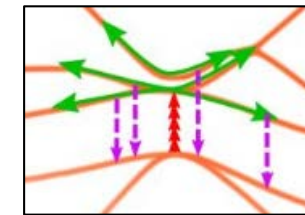
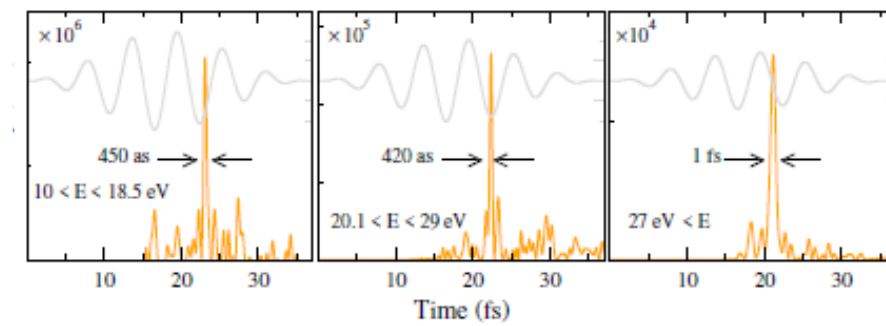
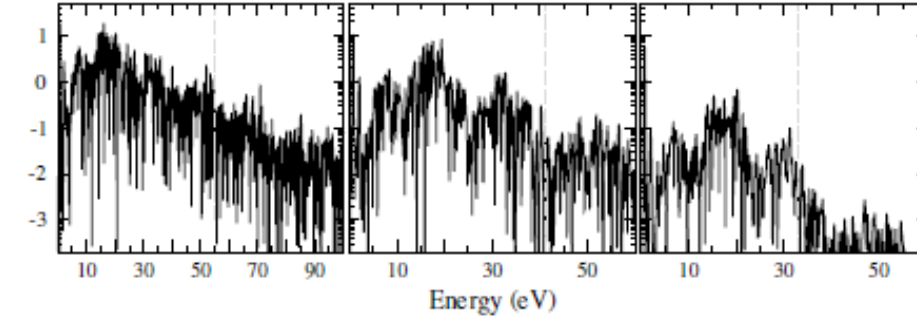
(a) $f=2, c=2, \phi_2=0 \text{ rad}$ (b) $f=2.1, c=2, \phi_2=5 \text{ rad}$ (d) $f=2, c=1.1, \phi_2=1 \text{ rad}$ (c) $f=2.1, c=1, \phi_2=0 \text{ rad}$ (e) $f=2, c=0.44, \phi_2=5.5 \text{ rad}$



one-color pulses

$E_{peak} = 1.4 \text{ V/\AA}$ ← → 0.9 V/\AA

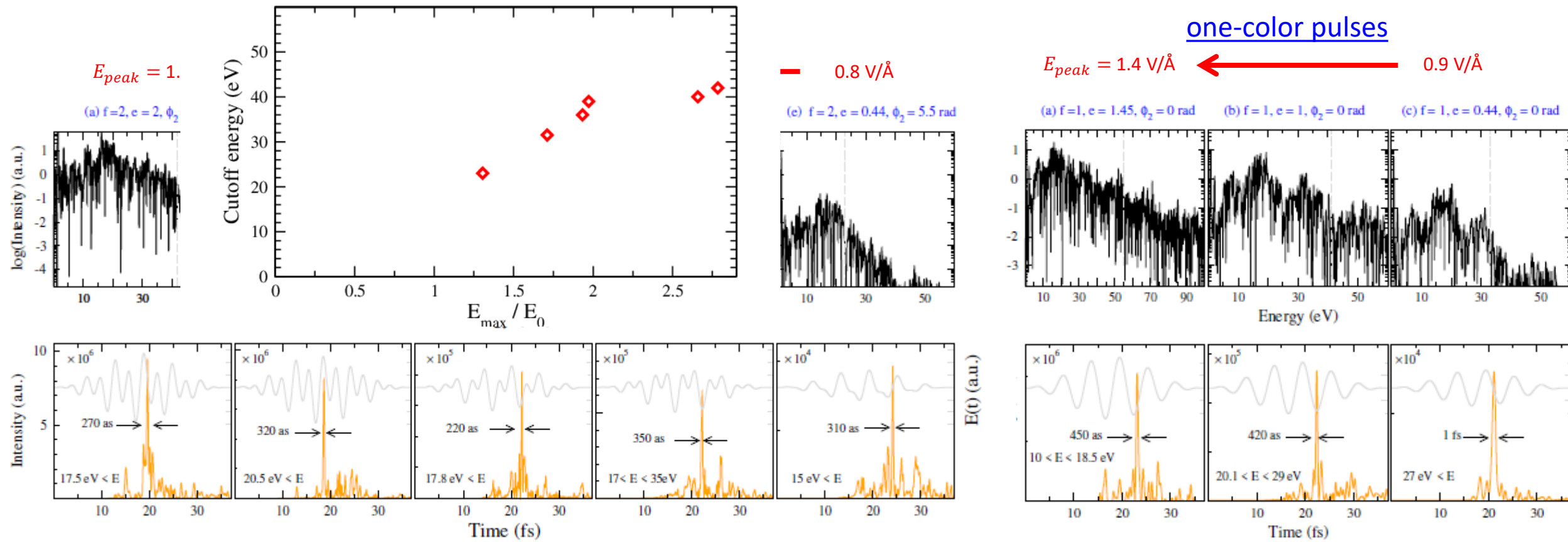
(a) $f=1, c=1.45, \phi_2=0 \text{ rad}$ (b) $f=1, c=1, \phi_2=0 \text{ rad}$ (c) $f=1, c=0.44, \phi_2=0 \text{ rad}$



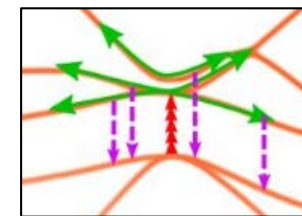
- IAP duration for two-color pulses shows no serious dependence to electric field strength which reveals the **importance of asymmetric pulse in IAP generation**.
- Shorter IAPs and wider band width for two-color pulses
- Electric field enhancement increases the brightness of IAPs as well as HHG cutoff energy
- Asymmetric pulses yield shorter energy cutoff than single-color pulses

|electric field| ↑ → band structure curvature ↑ → intraband dynamics ↑

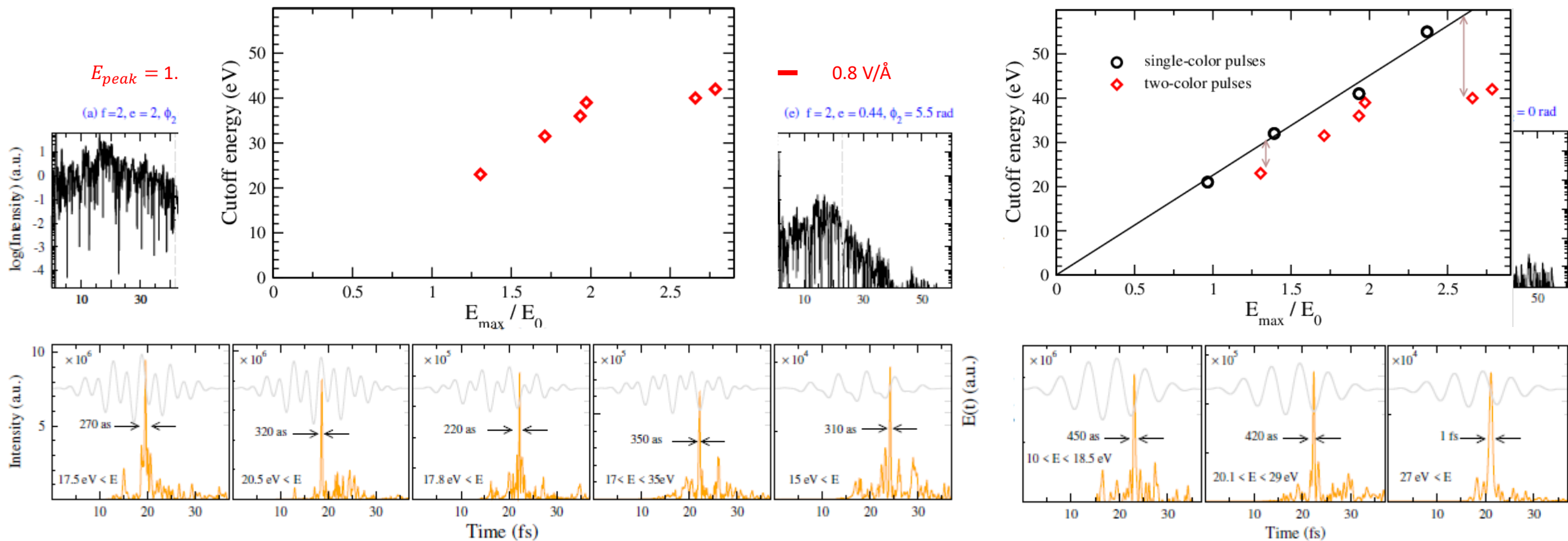
|vector potential| ↑ → band gap ↑ → interband dynamics ↑



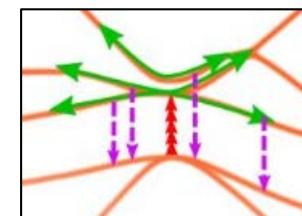
- ➔ IAP duration for two-color pulses shows no serious dependence to electric field strength which reveals the **importance of asymmetric pulse in IAP generation**.
- ➔ Shorter IAPs and wider band width for two-color pulses
- ➔ Electric field enhancement increases the brightness of IAPs as well as HHG cutoff energy
- ➔ Asymmetric pulses yield shorter energy cutoff than single-color pulses



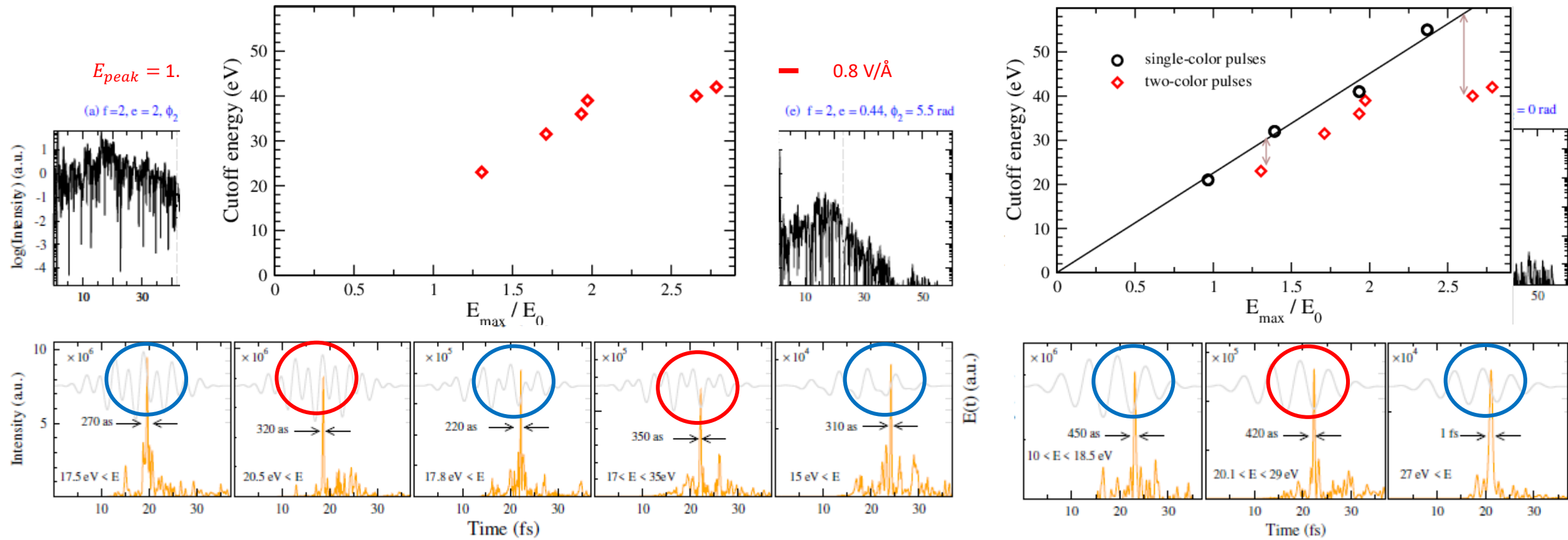
$|\text{electric field}| \uparrow \rightarrow \text{band structure curvature} \uparrow \rightarrow \text{intraband dynamics} \uparrow$
 $|\text{vector potential}| \uparrow \rightarrow \text{band gap} \uparrow \rightarrow \text{interband dynamics} \uparrow$



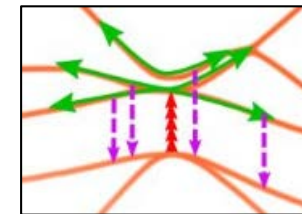
- IAP duration for two-color pulses shows no serious dependence to electric field strength which reveals the **importance of asymmetric pulse in IAP generation**.
- Shorter IAPs and wider band width for two-color pulses
- Electric field enhancement increases the brightness of IAPs as well as HHG cutoff energy
- Asymmetric pulses yield shorter energy cutoff than single-color pulses



$|\text{electric field}| \uparrow \rightarrow \text{band structure curvature} \uparrow \rightarrow \text{intraband dynamics} \uparrow$
 $|\text{vector potential}| \uparrow \rightarrow \text{band gap} \uparrow \rightarrow \text{interband dynamics} \uparrow$



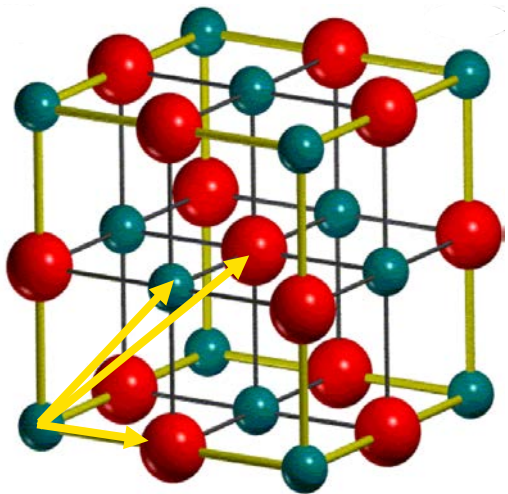
- IAP duration for two-color pulses shows no serious dependence to electric field strength which reveals the **importance of asymmetric pulse in IAP generation.**
- Shorter IAPs and wider band width for two-color pulses
- Electric field enhancement increases the brightness of IAPs as well as HHG cutoff energy
- Asymmetric pulses yield shorter cutoff energy than single-color pulses



$|\text{electric field}| \uparrow \rightarrow \text{band structure curvature} \uparrow \rightarrow \text{intraband dynamics} \uparrow$
 $|\text{vector potential}| \uparrow \rightarrow \text{band gap} \uparrow \rightarrow \text{interband dynamics} \uparrow$

linearly polarized pulse: Anisotropy impacts

$$\vec{A}(t) = \vec{A}_0 \sin^2(t/\delta) [\sin(\omega t) + 1/2 \times \sin(2\omega t + 1)]$$

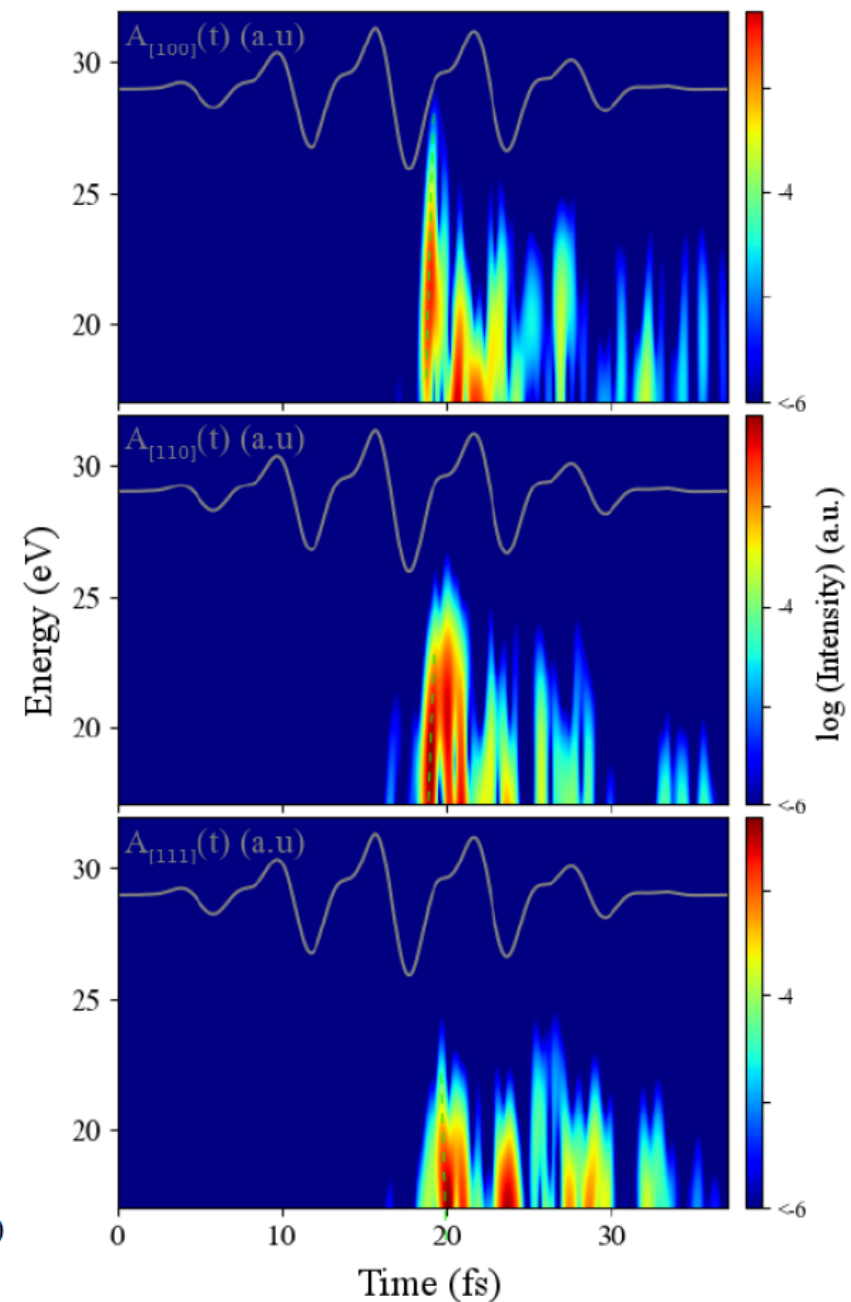
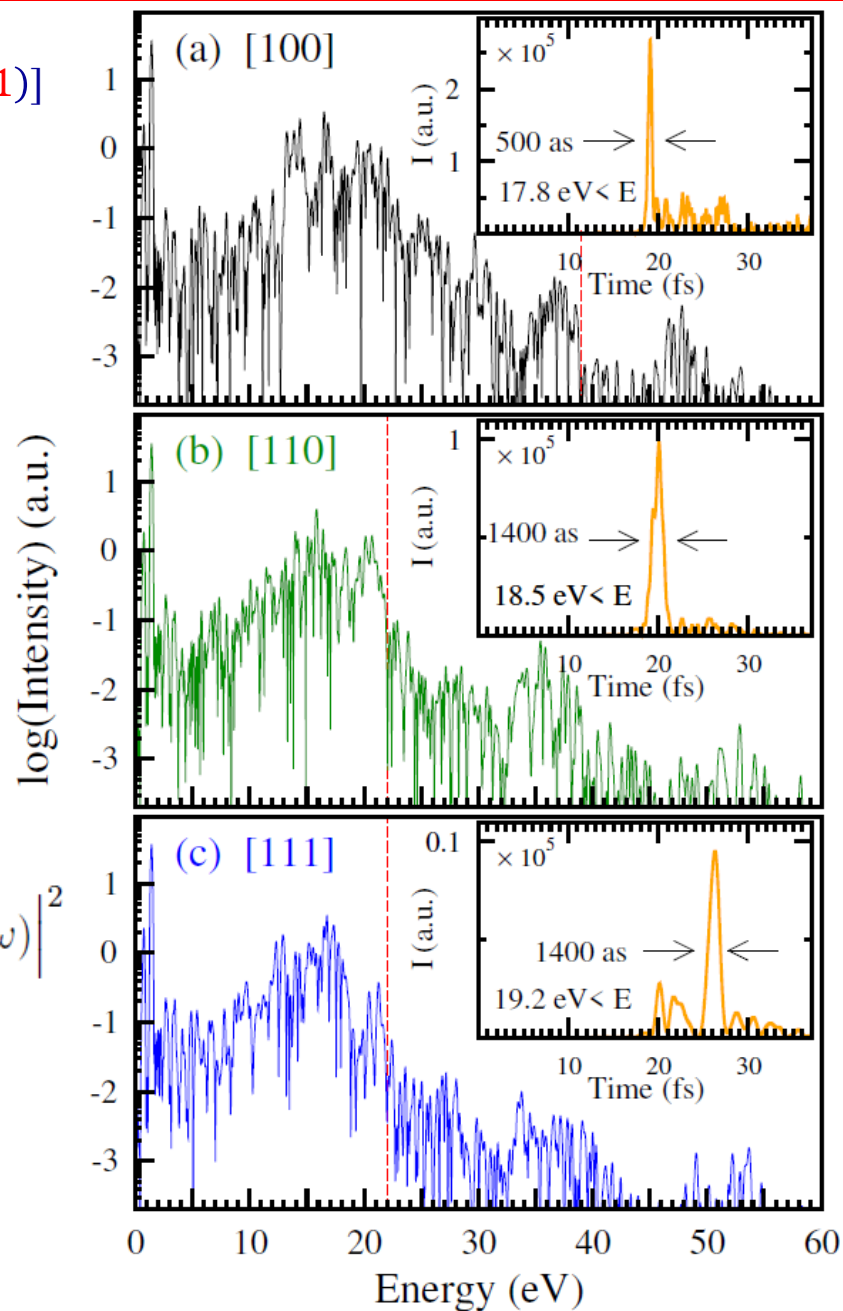


- ➔ Stronger HHG/more efficient IAP for [100] polarized pulse

$$HHG \propto \left| FT \left(\int_{\Omega} d\mathbf{r} n(\mathbf{r}, t) \nabla v_{\text{nuc}}(\mathbf{r}) \right) + N_e E(\omega) \right|^2$$

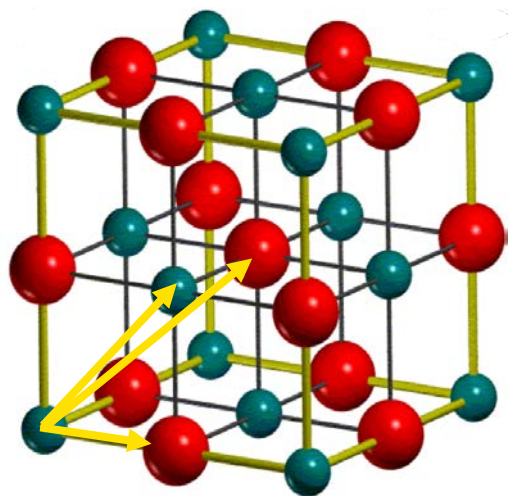
Phys. Rev. Lett. 118, 087403 (2017).

- ➔ Addition to the pulse asymmetry, IAP are strongly influenced by the crystal orientation.
- ➔ Attochirp appearance: illustration of the complex attosecond dynamics occurring within the MgO bands.



linearly polarized pulse: Anisotropy impacts

$$\vec{A}(t) = \vec{A}_0 \sin^2(t/\delta) [\sin(\omega t) + 1/2 \times \sin(2\omega t + 1)]$$

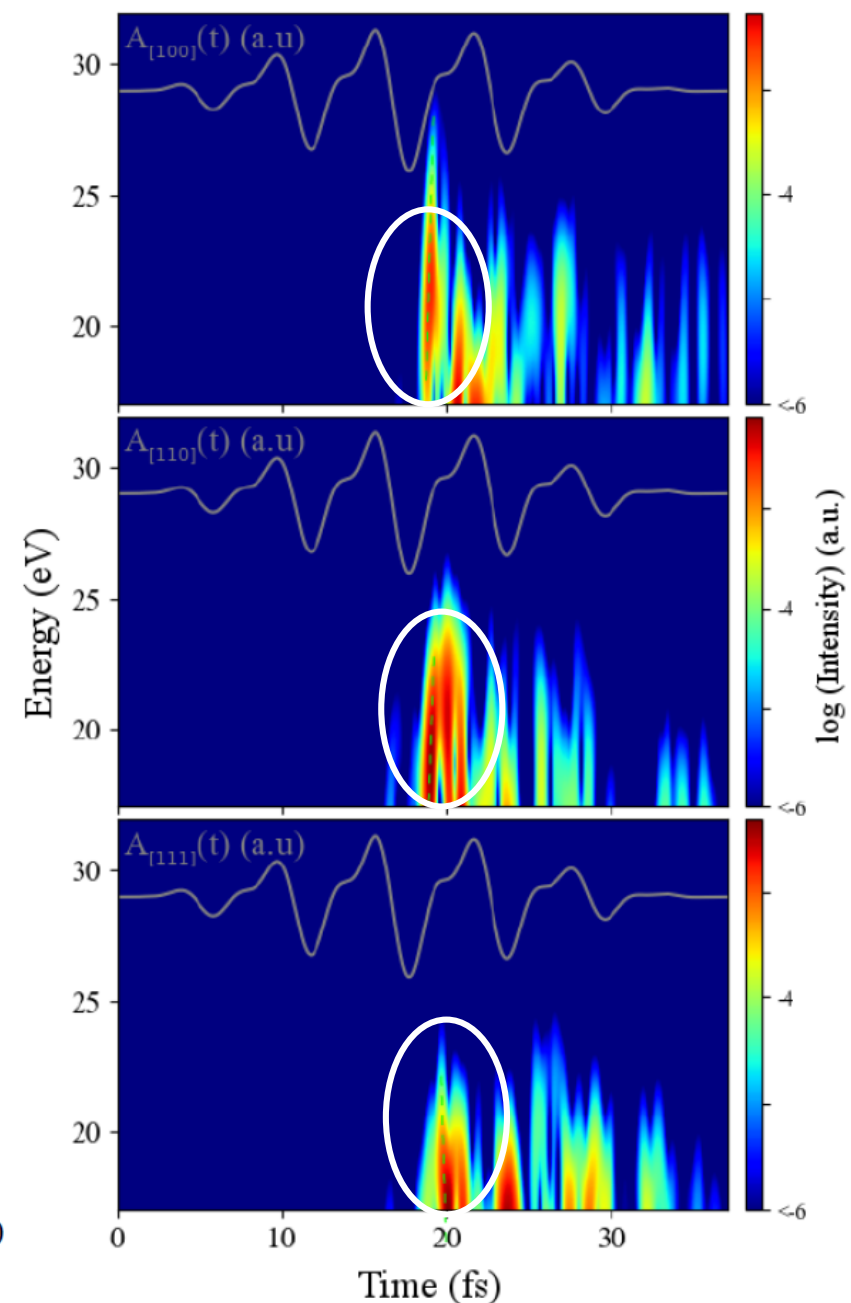
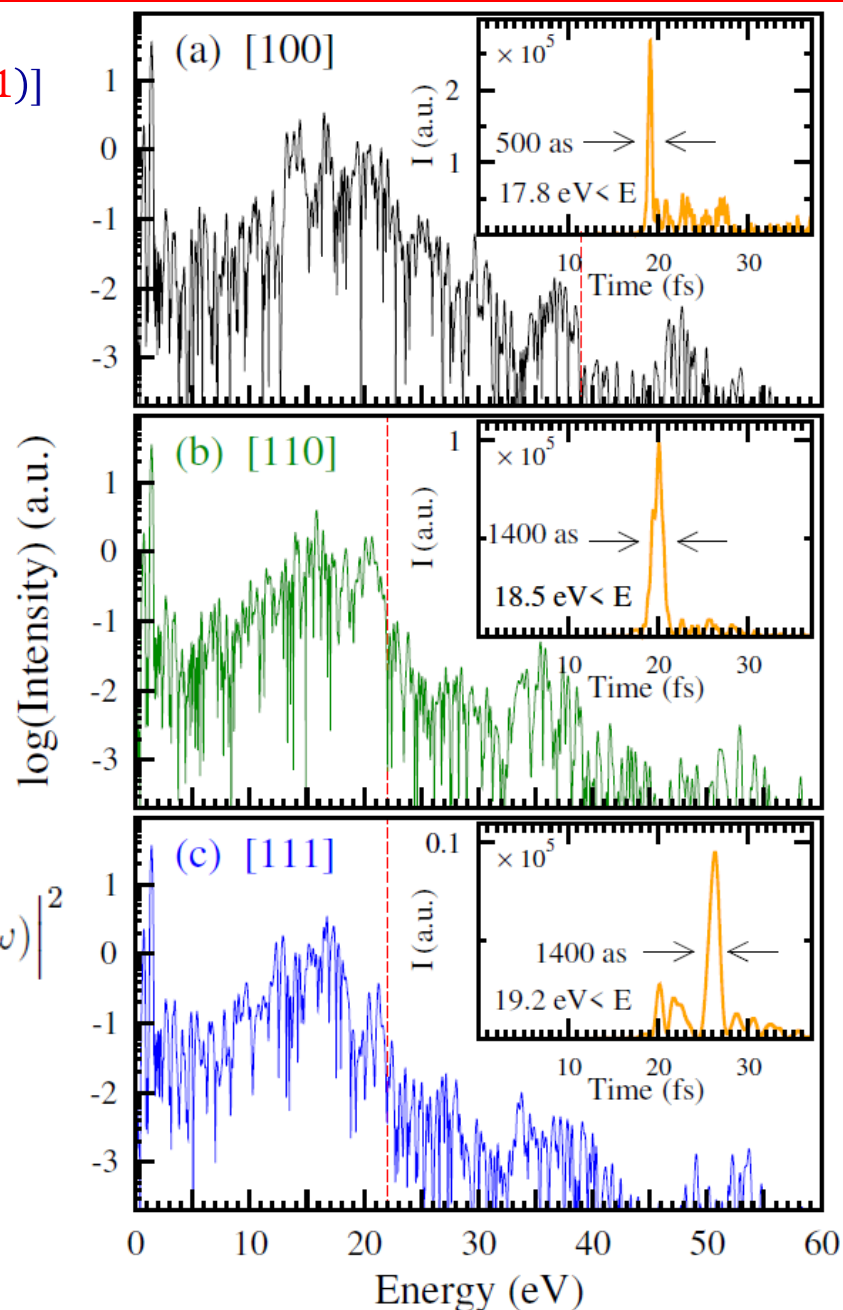


- ➔ Stronger HHG/more efficient IAP for [100] polarized pulse

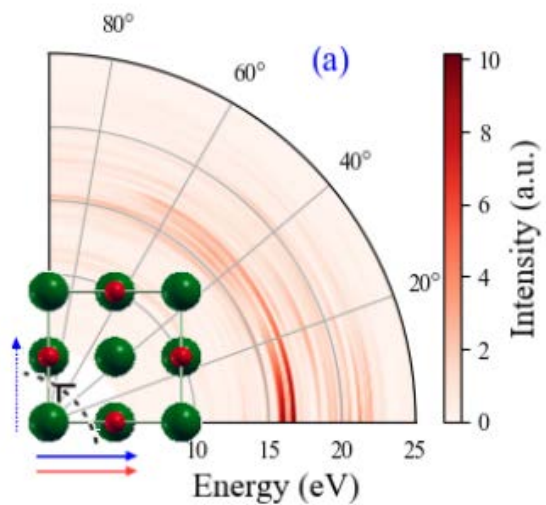
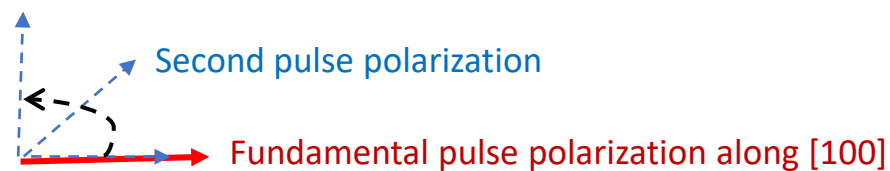
$$HHG \propto \left| FT \left(\int_{\Omega} d\mathbf{r} n(\mathbf{r}, t) \nabla v_{\text{nuc}}(\mathbf{r}) \right) + N_e E(\omega) \right|^2$$

Phys. Rev. Lett. 118, 087403 (2017).

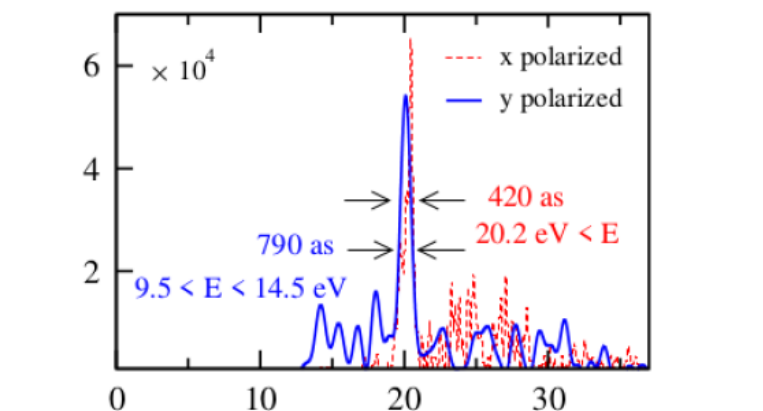
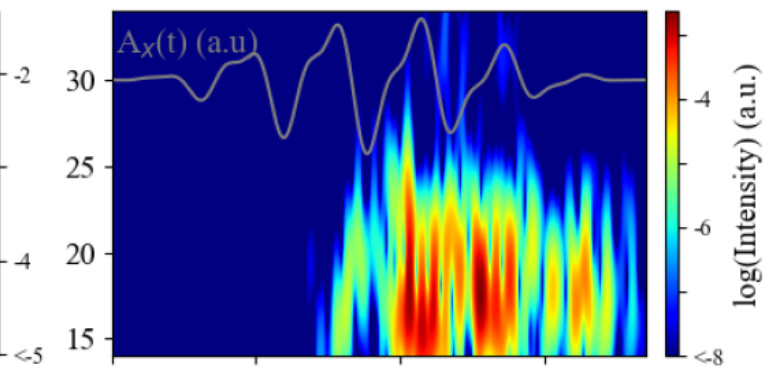
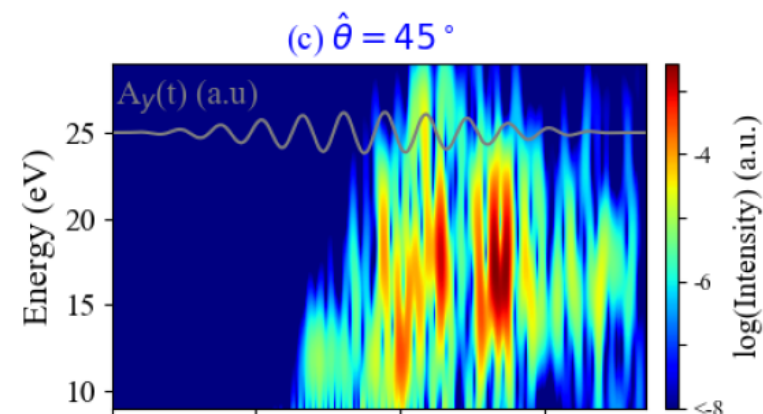
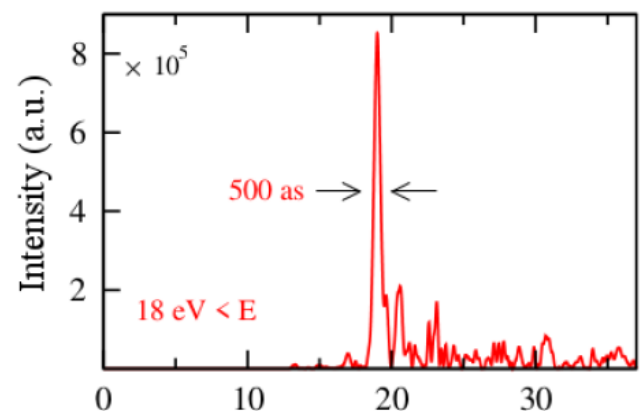
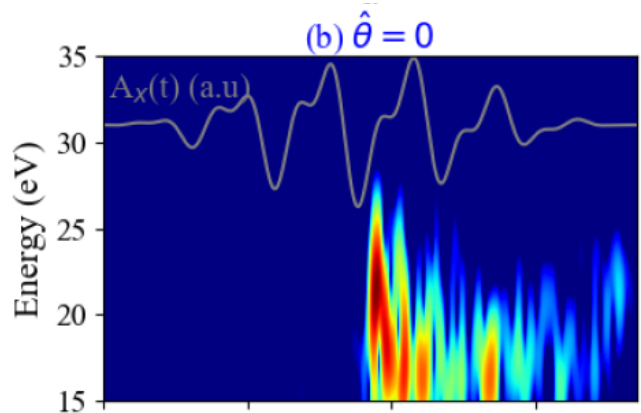
- ➔ Addition to the pulse asymmetry, IAP are strongly influenced by the crystal orientation.
- ➔ Attochirp appearance: illustration of the complex attosecond dynamics occurring within the MgO bands.



$$\vec{A}(t) = A_0 \sin^2(t\pi/\delta) [\sin(\omega_0 t) \hat{i} + \frac{1}{2.1} \sin(2.1\omega_0 t + 5.5) \hat{\theta}]$$



$\hat{\theta}$	Cutoff energy
0	36 eV
45°	27 eV
90°	25 eV



Time (fs)

TD-DFT calculations of the time evolution of the electronic wave functions are performed using octopus code

Extracting IAPs as short as ~ 200 - 300 as from the harmonic emission in EUV range from MgO

Anisotropic behavior of MgO harmonic emissions, and stronger HHG/more efficient IAP for [100] light polarized.

Linear dependence of cutoff energy to the driving laser peak field and independency of cutoff to the pulse wavelength.



Rapidly dropping of HHG signals for the elliptical polarized pulses, but providing elliptically polarized IAPs.

Attochirp appearance for harmonics between 15-21 eV with presenting a plateau in the HHG spectrum, and the lying conduction bands in the band structure

Our work prepares future all solid-state compact optical devices offering perspectives beyond traditional IAP emitted from atoms.

More details will be found in *High harmonics and isolated attosecond pulses from MgO*, Z. Nourbakhsh, et al. ([arXiv:2010.08010v1](https://arxiv.org/abs/2010.08010v1))

Thank you for your attention